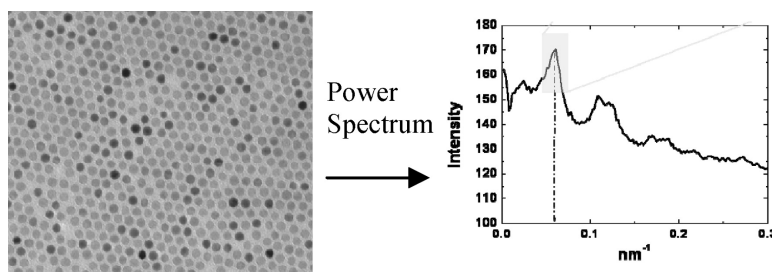Article

Functional Oligomers for the Control and Fixation of Spatial Organization in Nanoparticle Assemblies

Chun-Kwei Wu, Kristi L. Hultman, Stephen O'Brien, and Jeffrey T. Koberstein

Power Spectrum

More About This Article

Additional resources and features associated with this article are available within the HTML version:

- Supporting Information
- Access to high resolution figures
- Links to articles and content related to this article
- Copyright permission to reproduce figures and/or text from this article

View the Full Text HTML

Functional Oligomers for the Control and Fixation of Spatial Organization in Nanoparticle Assemblies

Chun-Kwei Wu,[†] Kristi L. Hultman,[‡] Stephen O'Brien,[‡] and Jeffrey T. Koberstein*,[†]

Departments of Chemical Engineering and of Applied Physics and Applied Mathematics, Materials Research Science and Engineering Center, Columbia University, New York, New York 10027

Received October 3, 2007; E-mail: jk1191@columbia.edu

Abstract: Interactions in nanoparticle assemblies play an important role in modulating their interesting magnetic and optical properties. Controlling and fixing the distance between nanoparticles is therefore crucial to the development of next-generation nanodevices. Here, we show that the interparticle distance in two-dimensional assemblies can be quantitatively controlled by functionalizing the nanoparticles with short polymers containing one functional end group that binds to the nanoparticle. Carboxy-functional poly-(dimethylsiloxane) (PDMS) ligands are attached to the nanoparticle surface by a simple ligand exchange process with the oleic acid synthesis ligands. The distance between nanoparticles is manipulated by adjusting either the number of PDMS ligands per molecule or their molecular weight. The use of PDMS ligands is unique in that they provide a means to permanently and robustly fix the spatial distribution of nanoparticles because PDMS is readily converted to silicon oxide by a simple UV/ozone treatment. The distance between nanoparticles can be designed a priori, as it is found to scale well with theoretical predictions for the thickness of the surface-bound polymer brush layer.

It is well-established that individual nanoparticles can exhibit unique size-dependent electronic, optical, magnetic, and photonic properties.[1] In practice, however, nanoparticles must usually be imbedded in some matrix for these properties to be practical. It has become apparent that the properties of nanoparticle assemblies can differ from those of the neat nanoparticles. If the interparticle distance is appropriate to encourage nanoscale cooperative processes[2] such as electron tunneling, dipolar coupling, and Forster energy transfer, photonic and electronic properties can be can be manipulated by controlling the distance between nanoparticles. In some cases, altogether new properties based upon collective nanoparticle behavior will ensue. The realization of these properties in next-generation applications including catalysis,[3,4] optoelectronics,[5] sensors,[6] and medicine[7,8] therefore requires methods for the precise spatial assembly of nanoparticles.

Some progress has already been made in the development of self-organizing nanoparticle assemblies. The distance between nanoparticles has been controlled by grafting polymers to[9] or polymerizing polymers from[10] the nanoparticle surfaces, or by using a number of functional molecules, including alkanethiols,[11] dendrimers,[12] proteins,[13] DNA,[14] or difunctional linkers,[15,16] to mediate the nanoparticle self-assembly process. It has been demonstrated that magnetic properties can be manipulated in assemblies of superparamagnetic particles by using dendrimers to mediate the interparticle distances.[17] Here we show that end-functional oligomers of poly(dimethylsiloxane) (PDMS) tethered by their ends to the nanoparticle surfaces, hereafter referred to as ligands, are an effective means to control the distance between particles over a length scale of a few nanometers, precisely the scale over which dipolar interactions and cooperative processes such as electron tunneling and energy transfer are known to occur.

While polymers have already been employed as ligands to control nanoparticle spatial distribution, we demonstrate that the use of PDMS as a ligand material has several unique advantages. First, end-functional PDMS in the oligomeric molecular weight range is commercially available and generally

---

[†] Department of Chemical Engineering.

[‡] Department of Applied Physics and Applied Mathematics.

(1) Shenhar, R.; Norsten, R. B.; Rotello, V. M. *Adv. Mater.* **2005**, *17*, 657−669.

(2) Murray, C. B.; Kagan, C. R.; Bawendi, M. G. *Annu. Rev. Mater. Sci.* **2000**, *20*, 545−610.

(3) Lewis, L. N. *Chem. Rev.* **1993**, *93*, 2693−2730.

(4) Kong, J.; Cassell, A. M.; Dai, H. *Chem. Phys. Lett.* **1998**, *292*, 567−574.

(5) Trindade, T.; O'Brien, P.; Pickett, N. L. *Chem. Mater.* **2001**, *13*, 3843−3858.

(6) Shipway, A. N.; Katz, E.; Willner, I. *Chem. Phys. Chem.* **2000**, *1*, 18−52.

(7) Wilson, K. S.; Goff, J. D.; Riffle, J. S.; Harris, L. A.; St. Pierre, T. G. *Polym. Adv. Technol.* **2005**, *16*, 200−211.

(8) Dailey, J. P.; Phillips, J. P.; Li, C.; Riffle, J. S. *J. Magn. Magn. Mater.* **1999**, *194*, 140.

(9) Yockell-Lelievre, H.; Desbiens, J.; Ritcey, A. M. *Langmuir* **2007**, *23*, 2843−2850.

(10) Matsuno, R.; Otsuka, H.; Takahara, H. *Soft Matter* **2006**, *2*, 415−421.

(11) Motte, L.; Pileni, P. M. *J. Phys. Chem. B* **1998**, *102*, 4104−4109.

(12) Frankamp, B. L.; Boal, A. K.; Rotello, V. M. *J. Am. Chem. Soc.* **2002**, *124*, 15146−15147.

(13) Verma, A.; Srivastava, S.; Rotello, V. M. *Chem. Mater.* **2005**, *17*, 6317−6322.

(14) Srivastava, S.; Samanta, B.; Arumugam, P.; Han, G.; Rotello, V. M. *J. Mater. Chem.* **2007**, *17*, 52−55.

(15) Chen, S. *Langmuir* **2001**, *17*, 2878−2884.

(16) Sidhaye, D. S.; Kashyap, S.; Sastry, M.; Hotha, S.; Prasad, B. L. V. *Langmuir* **2005**, *21*, 7979−7984.

(17) Frankamp, B. L.; Boal, A. K.; Tuominen, M. T.; Rotello, V. M. *J. Am. Chem. Soc.* **2005**, *127*, 9731−9735.

provides for interparticle distances that are more conducive to interparticle interactions than higher molecular weight polymer. Second, PDMS ligands provide a means to permanently fix the spatial distribution of nanoparticles within a film. When treated with oxygen plasma[18] or UV/ozone[19] processes, PDMS is converted into silicon oxide, SiO_x. The resultant assemblies of nanoparticles embedded in silicon oxide are inherently more robust than nanoparticle assemblies embedded in organic or polymeric ligands. They are intrinsically more temperature-resistant, do not swell or dissolve in organic solvents, and should be more resistant to wear due to the increased hardness of silicon oxide.[20] Finally, the ability to create assemblies of nanoparticles embedded in silicon oxide with controllable interparticle distance enables an entirely new set of applications. Silicon oxide is known to have interesting membrane separation properties.[18,21] Embedding nanoparticles into a thin film of silicon oxide has already been demonstrate to constitute an interesting route to gas separation membranes[22] with improved permeability and stability against water vapor.

Results

Polymeric ligands are tethered by their ends to the nanoparticle surface by a straightforward ligand exchange process (described in detail in the Supporting Information). The nanoparticles used for this illustration, iron oxide (γ-Fe_2O_3) with diameters (d) of 5.4, 9.5, and 13.5 nm, are prepared with oleic acid capping ligands. The polymeric ligands employed are commercially available (from Polymer Source) low molecular weight poly(dimethyl siloxane) (PDMS) terminated on one end with a carboxylic acid group (See Supporting Information Figure 1). Low molecular weight polymeric ligands are desirable to ensure that the interparticle distances lie within an appropriate range (i.e., several nanometers) for the promotion of interparticle processes such as energy transfer and electron tunneling. The three PDMS ligands employed, therefore, are chosen to be within the oligomeric range with nominal number average molecular weights (M_n) of 1000, 5000, and 10 000. Characterization results appear in Supporting Information Table 1. The success of polymer ligand exchange is confirmed by infrared spectroscopic measurements and dynamic light scattering analysis summarized in Supporting Information Figures 2 and 3.

The surface areal densities (σ) of PDMS ligands on the nanoparticles were estimated by thermal gravimetric analysis (TGA) in a reductive environment as described in Supporting Information Figures 4−6. Under these conditions, the PDMS surface ligands are removed; however, the iron oxide undergoes multiple reduction steps as indicated by the TGA results in Supporting Information Figure 4. The occurrence of oxide reduction complicates the analysis, but the polymer grafting density can be obtained by assuming that oxide reduction in the nanoparticle assemblies occurs in the same way as is observed in Supporting Information Figure 4 for pure iron oxide. We have therefore made no attempt to examine the nature of oxide reduction in any detail. The ligand areal density can also

(18) Houston, K. S.; Weinkauf, D. H.; Stewart, F. F. *J. Membr. Sci.* **2002**, *205*, 103−112.
(19) Mirley, C. L.; Koberstein, J. T. *Langmuir* **1995**, *11*, 1049−1052.
(20) Archard, J. F. *J. Appl. Phys.* **1953**, *24*, 981−988.
(21) Ouyang, M.; Muisener, R. J.; Boulares, A.; Koberstein, J. T. *J. Membr. Sci.* **2000**, *177*, 177−187.
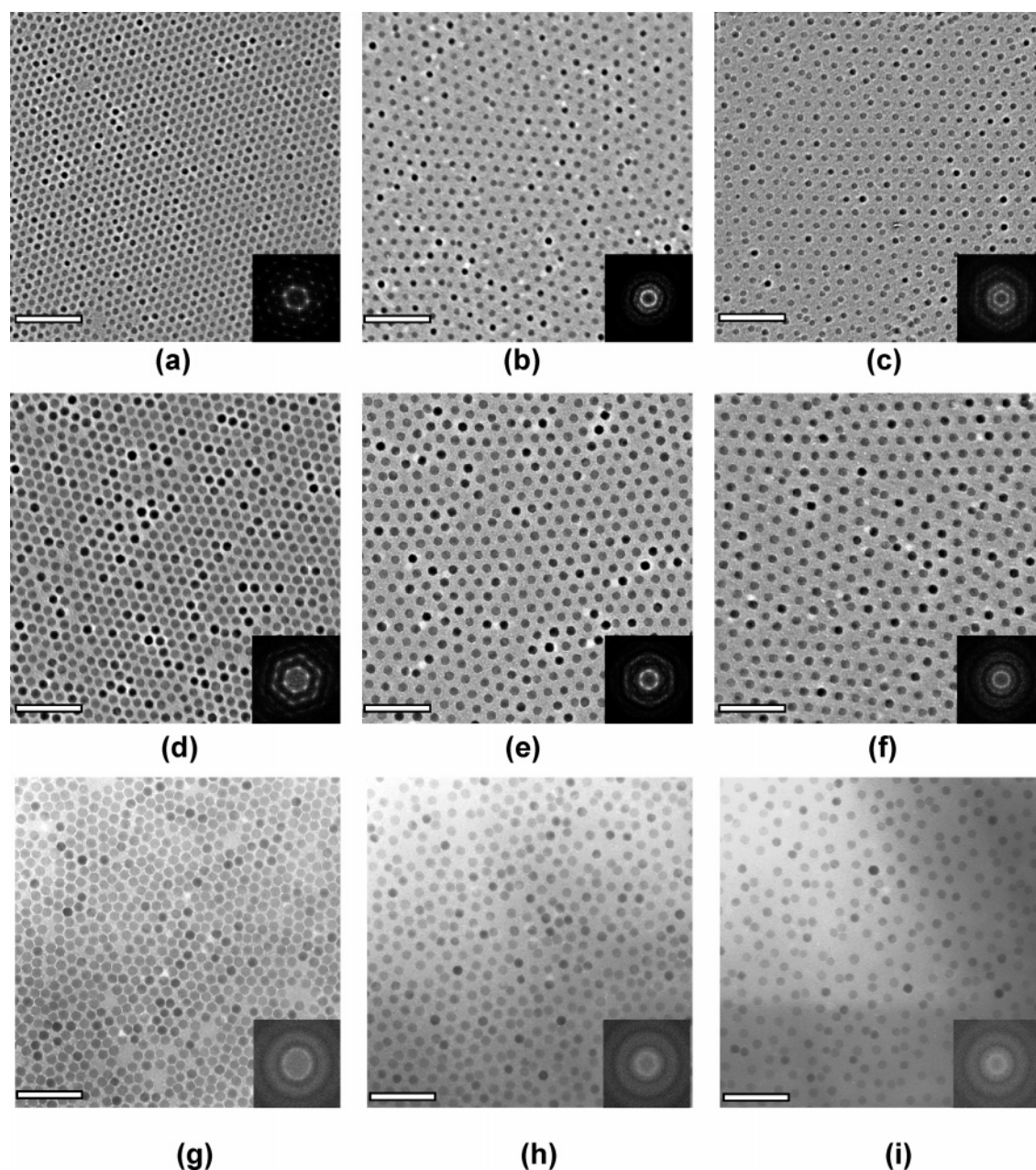(22) Asaeda, M.; Sakou, Y.; Yang, J.; Shimasaki, K. *J. Membr. Sci.* **2002**, *209*, 163−175.

Table 1. Grafting Densities of PDMS Ligands on Fe_2O_3 Nanoparticles[a]

| | $d = 13.5$ nm | | $d = 9.5$ nm |
M_n PDMS	TGA	packing model	packing model
1000	4.0 ± 1.3	5.2 ± 0.2	5.9 ± 0.2
5000	3.1 ± 1.3	2.5 ± 0.2	2.6 ± 0.1
10000	2.7 ± 1.4	2.1 ± 0.2	2.6 ± 0.3

[a] Determined by TGA and calculated from the interparticle separation distance by application of the hexagonal packing model; given in ligands per square nanometer.

be calculated from the measured interparticle separation distance by application of the two-dimensional packing model shown schematically in Supporting Information Figure 7: volume-filling hexagonally packed ligand-coated nanoparticles within a film of thickness equal to the interparticle separation distance. The model calculations are described in Supporting Information eqs S.1 and S.2, and the resultant grafting densities are listed in Table 1. The ligand densities for the 9.5 nm particles determined by the two methods are in agreement within experimental error.

Monolayer assemblies of the PDMS-modified Fe_2O_3 nanoparticles are made by depositing a solution of ligand-modified nanoparticles onto a substrate for transmission electron microscopic (TEM) analysis followed by evaporation. The results are indistinguishable for monolayer films obtained by spin coating. It is evident from Figure 1 (micrographs a−c and d−f) that the interparticle separation in the thin composite films increases monotonically with the length of the polymeric ligand. The insets in the figures are the 2D FFT power spectra of the corresponding TEM images. The average interparticle separation distance, l, is determined from the positions of maxima in the 2D FFT power spectrum.

Correlation lengths that describe the distance over which the hexagonal order persists can be determined by analyses of the 2D autocorrelation function for the TEM images. The decay in the correlation function is well described by an exponential decay function with correlation length ξ. The regularity of nanoparticle periodicity is reflected in the number of lattice repeats (Φ) within the correlation length: $\xi = \Phi l$. The l, Φ, and ξ values obtained for the PDMS-modified Fe_2O_3 arrays are summarized in Table 2. The interparticle separation distance follows an approximately linear dependence on polymer chain length; however, the particles become less ordered (that is, the correlation length decreases) with increasing ligand chain length. Supporting Information Figures 10 and 11 describe the procedures used for analyses of the power spectra and correlation functions.

The spatial distribution of nanoparticles in the monolayers is permanently fixed by converting the PDMS ligands to SiO_x, a transformation accomplished by exposure to UV/ozone at atmospheric conditions. Successful transformation is confirmed by the results presented in Supporting Information Table 3 and Supporting Information Figures 8 and 9. After conversion, the resultant films are single-nanoparticle dispersions of iron oxide within a matrix of SiO_x, as shown in Figure 1 parts g−i. The regularity of packing in the structures is reduced after conversion, however, because the transformation reaction from PDMS to SiO_x is accompanied by volume shrinkage. The thicknesses of Langmuir−Blodgett films of PDMS, for example, were found to decrease by 50% after UV/ozone treatment.[19] Quantitative

Figure 1. TEM images of two-dimensional PDMS-modified Fe_2O_3 nanoparticle assemblies: (a) $d = 9.5$ nm, $M_n = 1K$; (b) $d = 9.5$ nm, $M_n = 5K$; (c) $d = 9.5$ nm, $M_n = 10K$; (d) $d = 12.5$ nm, $M_n = 1K$; (e) $d = 12.5$ nm, $M_n = 5K$; (f) $d = 12.5$ nm, $M_n = 10K$; (g) $d = 12.5$ nm, $M_n = 1K$, after UV/O_3; (h) $d = 12.5$ nm, $M_n = 5K$, after UV/O_3; (i) $d = 12.5$ nm, $M_n = 10K$, after UV/O_3. (Insets) 2D FFT power spectra. Scale bars indicate 100 nm.

Table 2. Interparticle Spacing l, Correlation Length ξ, and Number of Correlated Repeat Units Φ in PDMS-Modified Fe_2O_3 Composite Films

M_n PDMS	d (nm)	l (nm)	ξ (nm)	Φ
1000	9.5	15.7 ± 0.2	33.7 ± 0.7	2.15 ± 0.05
1000	13.5	19.5 ± 0.2	47 ± 0.9	2.41 ± 0.05
1000 UV/ozone	13.5	19.3	12	0.62
5000	9.5	19.8 ± 0.3	33.2 ± 0.6	1.67 ± 0.04
5000	13.5	25.1 ± 0.6	46 ± 0.9	1.83 ± 0.06
5000 UV/ozone	13.5	26.8	10.5	0.42
10 000	9.5	24.7 ± 0.9	39.1 ± 0.8	1.58 ± 0.06
10 000	13.5	29.4 ± 0.8	29.5 ± 0.6	1.00 ± 0.03
10 000 UV/ozone	13.5	31.7	13.7	0.46

analysis of the TEM images shows that the interparticle separation distances are relatively unchanged by the conversion process but the correlation lengths decrease significantly, as illustrated in Table 2.

Discussion

The grafting densities (Table 1) decrease with increasing ligand molecular weight, indicating the adoption of more loosely packed PDMS configurations for higher molecular weights. A similar trend was found for close-packed Langmuir−Blodgett films of PDMS-COOH.[23] A decrease in grafting density with increasing molecular weight is also found for polymer brushes prepared by the "grafting to" method due to configurational entropy effects. The degree of spatial order also decreases with

(23) Lenk, T. L.; Lee, D. H. T.; Koberstein, J. T. *Langmuir* **1994**, *10*, 1857−1864.

increasing ligand molecular weight, most likely due to the decrease in steric confinement effects experienced by longer chains farther from the nanoparticle surface.

The most important question to answer is whether the interparticle separation can be controlled and predicted. The interparticle separation is primarily determined by the configurations of the polymeric ligands that are end-tethered to the nanoparticle surface. Such polymers are generally termed polymer brushes and have been the subject of a large number of theoretical treatments using scaling analysis,[24,25] self-consistent field calculations (SCF),[26,27] and Monte Carlo[27] and molecular dynamics simulations.[28]

The Alexander[24] and de Gennes[25] scaling model for polymer brushes predicts that the height of a planar brush in a good solvent (h_g) scales as $h_g \sim N\sigma^{1/3}$, where N is the degree of polymerization for the grafted polymer. Daoud and Cotton[29] extended the free energy scaling approach to polymers tethered by their ends onto a convex spherical grafting surface, and Birshtein et al.[30] considered grafting onto a cylindrical surface. The generalized scaling prediction for brush height in a good solvent is

$$h_g \equiv aN^{[3/(3+D)]}\sigma^{[1/(3+D)]}\left(\frac{r}{a}\right)^{[3/(3+D)]} \qquad (1)$$

where $D = 0$, 1, or 2 for planar, cylindrical, or spherical surfaces, respectively, for brushes adsorbed onto a convex surface of radius r. Birshtein and Zhulina[31,32] concluded that the height of a brush grafted to a spherical surface in a θ solvent scaled as

$$h_\theta \sim N^{1/2}\sigma^{1/4}r^{1/2} \qquad (2)$$

To investigate whether the spherical brush model can predict the packing of nanoparticles in the absence of solvent (i.e., corresponding to the θ state), we adopt the scaling theory for a spherical brush in θ solvent. Figure 2 demonstrates that the apparent experimental brush height, $h_\theta = (l - d)/2$, does scale as $N_{PDMS}^{1/2}\sigma^{1/4}r^{1/2}$, as predicted by theory. The results calculated from experimental σ values (i.e., obtained directly from TGA measurements, ■) correspond well to the data calculated via the volume-filling hexagonal packing model (●), indicating that the PDMS-modified Fe_2O_3 films can be described as smooth films of constant thickness l, as assumed in this model. Areal densities obtained by application of the hexagonal packing model to data for the 9.5 nm modified nanoparticles (▲) also provide brush height scaling that is consistent with the spherical brush theory. Finally, the interparticle distances in films subject to the UV/ozone treatment (□) also follow the predicted scaling relationship. The difference in slope observed for the UV/ozone-treated samples may be due to the significant matrix shrinkage that occurs during the conversion of PDMS to silicon oxide. Since the interparticle separation distance is dependent directly
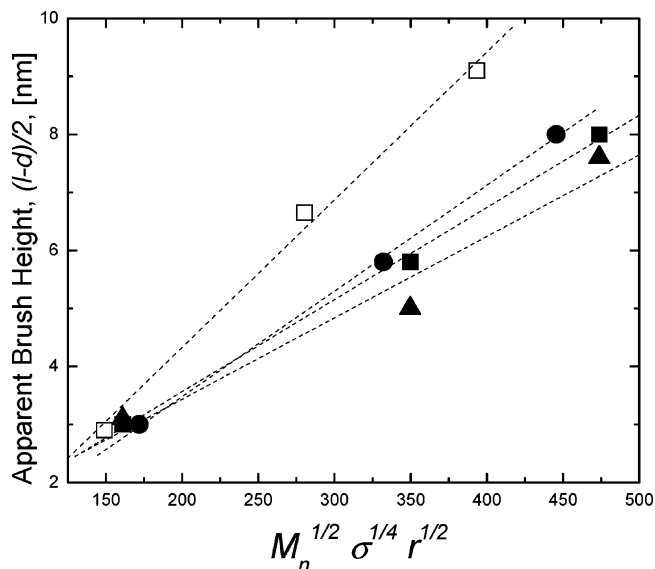
(24) Alexander, S. *J. Phys. (Paris)* **1977**, *38*, 983−987.
(25) de Gennes, P. G. *Macromolecules* **1980**, *13*, 1069−1075.
(26) Milner, S. T.; Witten, T. A.; Cates, M. E. *Macromolecules* **1988**, *21*, 2610−1619.
(27) Cosgrove, T.; Heath, T.; Van Lent, B.; Leermakers, F.; Scheutjens, J. *Macromolecules* **1987**, *20*, 1692−1696.
(28) Murat, M.; Grest, G. S. *Macromolecules* **1989**, *22*, 4054−4059.
(29) Daoud, M.; Cotton, J. P. *J. Phys. (Paris)* **1982**, *43*, 531−538.
(30) Birshtein, T. M.; Borisov, O. V.; Zhulina, E. B.; Khokhlov, A. R.; Yurasova, T. *Polym. Sci. U.S.S.R.* **1987**, *29*, 1293−1300.
(31) Birshtein, T. M.; Zhulina, E. B. *Polymer* **1984**, *25*, 1453−1461.
(32) Birshtein, T. M.; Zhulina, E. B.; Borisov, O. V. *Polymer* **1986**, *27*, 1078−1086.

Figure 2. Scaling representation of apparent brush height as a function of molecular weight and areal density of PDMS on γ-Fe_2O_3 nanoparticles. Areal density was determined from TGA on 13.5 nm particles (■), TGA after UV/ozone treatment on 13.5 nm particles (□), volume-filling hexagonal packing model on 13.5 nm particles (●), and volume-filling hexagonal packing model on 9.5 nm particles (▲). Dashed lines represent the results of linear regressions.

on the brush height, we can conclude that the interparticle separation scales as $l - d \approx M_n^{1/2}\sigma^{1/4}r^{1/2}$ and can therefore be readily controlled and predicted both for nanoparticles with PDMS ligands and for nanoparticles imbedded in silicon oxide.

Summary

The distance between γ-Fe_2O_3 nanoparticles in two-dimensional arrays is controlled by grafting low molecular weight, carboxy-terminated poly(dimethylsiloxane) (PDMS) ligands onto their surfaces. The PDMS-modified Fe_2O_3 hybrid nanoparticles spontaneously assemble from solution onto substrates to form hexagonally packed two-dimensional arrays. The distance between nanoparticles and a decay length describing the distance over which the nanoparticles are ordered are determined by image analyses of transmission electron microscope images of the nanoparticle assemblies. As the molecular weight of the PDMS ligand is increased, the interparticle separation distance increases and the regularity of packing decreases. The ligand grafting density is determined directly by thermal gravimetric analysis under reductive environment and agrees well with values calculated indirectly by analysis of the interparticle distance with a volume-filling hexagonal packing model. Comparison of experimental results with those obtained from the model calculations indicate that the two-dimensional nanoparticle composite films can be described as smooth volume-filling films of constant thickness l (i.e., equivalent to the interparticle separation distance), containing nanoparticles packed on a hexagonal lattice. The apparent thicknesses of the PDMS ligand layer bound to the nanoparticles, estimated from interparticles distances, are found to be about 3 times the radii of gyration of free PDMS, indicating that it is appropriate to treat the nanoparticle-bound ligands as a polymer brush. The apparent brush height is found to scale as $(l - d)/2 \approx M_n^{1/2}\sigma^{1/4}r^{1/2}$, in agreement with theoretical predictions for polymer brushes bound to spherical substrates. The distance

between particles in two-dimensional arrays therefore also scales as $l - d \approx M_n^{1/2}\sigma^{1/4}r^{1/2}$ and can be both controlled and predicted.

The nanoparticle arrays may be fixed or frozen in by converting the PDMS ligands to silicon oxide by exposing the assemblies to a UV/ozone environment. The average distance between particles remains roughly the same after transformation to silicon oxide, but the degree of hexagonal ordering is significantly reduced.

While we employ γ-Fe$_2$O$_3$ nanoparticles herein to demonstrate how PDMS-COOH ligands can be used to control and fix the distance between nanoparticles, the process presented is generally applicable to other metal oxide nanoparticles that have similar surface functionality, (i.e., metal-OH[33]) and should work for any nanoparticle if the appropriate polymer chain end is selected to adhere to the nanoparticle surface.

Supporting Information Available: Figures, tables, and equations as described in the text. This material is available free of charge via the Internet at http://pubs.acs.org.

JA077625I

(33) Wooding, A.; Kilner, M.; Lambrick, D. B. *J. Colloid Interface Sci.* **1991**, *144*, 236−242.